Fuel Communications 7 (2021) 100010

Contents lists available at ScienceDirect

Fuel Communications

journal homepage: www.elsevier.com/locate/jfueco

Retrofitting a high-speed marine engine to dual-fuel methanol-diesel operation: A comparison of multiple and single point methanol port injection

Jeroen Dierickx[a], Jip Verbiest[b], Tom Janvier[a], Jens Peeters[a], Louis Sileghem[a], Sebastian Verhelst[b,*]

[a] Ghent University, Belgium
[b] Lund University, Sweden

ARTICLE INFO

Article history:
Received 17 September 2020
Revised 29 January 2021
Accepted 27 February 2021

Keywords:
Dual-fuel operation
Methanol
Diesel
Retrofitting
Multiple point injection
Single point injection

ABSTRACT

As a result of climate change and increasingly stringent emission legislation the shipping industry has started with a transition to sustainable propulsion. Methanol is a viable fuel to reach this goal: it is a great engine fuel (high octane number, high heat of evaporation, and absence of carbon to carbon bonds) and a simple molecule that can be produced in a renewable way. The dual-fuel methanol-diesel technology with methanol injection in the intake has proven to be a promising retrofit solution for vessels. In this concept methanol injectors can be at multiple locations: single point injection (SPI) in the intake duct (assumed to be easier to install) or multiple point injection (MPI) at the intake ports of the cylinders (assumed to give additional in-cylinder cooling to suppress knock). This paper compares MPI and SPI with a focus on maximum methanol energy fraction (MEF), brake thermal efficiency (BTE) and NO_x emissions; and compares both injection modes with diesel-only operation. The highest MEF was measured in SPI: 84%. BTE was significantly higher in SPI for high MEFs due to a better combustion phasing resulting from higher intake temperatures. Higher intake temperatures in SPI resulted in higher NO_x emissions. Independent of the injection mode, NO_x mainly decreased compared to diesel-only operation. It is concluded that SPI is preferred from a cost point of view (maximizing BTE and minimizing retrofit cost) and that MPI is preferred from a sustainability point of view (maximizing MEF and minimizing NO_x emissions).

1. Introduction

Climate change awareness and increasingly stringent emission legislations have led to many conceptual ideas to change our energy landscape. A key design parameter for reaching such an energy transition is carbon neutral usage of our resources and this from cradle to grave. Power to gas or to liquid is one such a concept, and is mainly derived from the hydrogen or methanol economy as described and pioneered by George Olah et al. [1] (Olah, Goeppert, & Prakash, 2009). In this energy system renewable energy and circularity are crucial building blocks. Renewable energy can be liquefied or made gaseous and as such electricity is stored in a chemical. It can then be used as a base chemical for various day-to-day products, for energy storage, but also as a fuel for transportation. Hydrogen and methanol are two of these important chemicals, when used in transportation often referred to as e-fuels. Both fuels have been extensively studied in internal combustion engines [2] (Verhelst, Turner, Sileghem, & Vancoillie, 2019) [3] (Verhelst & Wallner, Hydrogen-fueled internal combustion engines, 2009), but mainly in spark ignition (SI) engines. Methanol has the advantage over hydrogen that it is a liquid at atmospheric conditions. This makes that the net volumetric energy density – which is the energy content per volume including the tank volume space – is more than 4 times higher for methanol than for hydrogen [4] (Pearson & Turner, 2012). This liquid state of methanol means less spacious storage and less complex fuel distribution systems. Methanol is furthermore a clean burning fuel, a simple molecule and one of the most traded chemicals worldwide. There-

Abbreviations: MPI, multiple point injection; SPI, single point injection; DF, dual-fuel; DO, diesel-only; HOF, high octane fuel; MEF, methanol energy fraction; MMF, methanol mass fraction; RR, replacement ratio; DSR, diesel substitution ratio; HRR, heat release rate; IMO, International Maritime Organization; PPRR, peak pressure rise rate; COV, coefficient of variation.

* Corresponding author.
E-mail address: sebastian.verhelst@energy.lth.se (S. Verhelst).

https://doi.org/10.1016/j.jfueco.2021.100010

fore it is seen as a viable marine fuel and alternative for crude oil based fuels in shipping.

One of the main challenges to implement methanol as a fuel results from the fact that in shipping the majority of the installed engines are compression ignition (CI) engines [5] (McGill, Remley, & Winther, 2013). However, methanol is a good fuel for SI engines because of its high octane number. Due to its low cetane number it is very challenging to use it directly in CI engines. Several solutions exist to overcome this problem: for example mixing methanol with diesel or adding ignition enhancers to methanol. The first has however limitations as methanol only mixes well in diesel (without additives) up to low fractions [6] (Yao, Pan, & Yao, 2017) [7] (Bechtold, Goodman, & Timbario, 2007). The second solution forms part of current engine research [2] (Verhelst, Turner, Sileghem, & Vancoillie, 2019) [8] (FASTWATER, 2020), but a main concern rises from the possible toxic behavior of ignition enhancers [6] (Yao, Pan, & Yao, 2017). A third solution, exploited in this research paper, is to use the dual-fuel technology. In this solution two fuels are used, one with a high cetane number to initiate the combustion (typically the original diesel) and one with a high octane number (such as methanol) that is ignited by the high cetane fuel. The dual-fuel technology knows different implementations depending on the injection position of the high octane fuel (HOF). The HOF can be injected directly in the cylinder, a technology chosen by Wärtsilä and MAN. Wärtsilä has proven its concept in their four stroke engine in the ferry demonstration project the Stena Germanica [9] (Stojcevski, Jay, & Vicenzi, 2016). The two stroke dual-fuel engines of MAN are available as a commercial product and are currently propelling nine methanol bunker vessels of Waterfront Shipping [10] (Mayer, Sjöholm, & Murakami, 2016). The HOF can also be injected at multiple points in the intake port directed at the intake valves, also called “fumigation”, and as such a mixture of fuel-air is sucked into the engine. This technology is chosen by for instance ABC Engines.

In 2019 the Horizon 2020 project LeanShips ended in which the fumigation technology was installed on a Volvo Penta D7C-B TA high-speed marine engine [11] (LeanShips, 2015–2019). The multiple point methanol injection (MPI) strategy was chosen as it is the least expensive dual-fuel solution of all because it enables low pressure methanol supply compared to high pressure methanol supply needed in the engine concepts employing direct cylinder injection. As a result, it does not require high pressure methanol injection in the cylinder (leading to difficult engine head adaptations). As such it is also an ideal retrofit solution, which is highly needed to make the shipping industry sustainable given the long average lifetime of vessels of 21 years [12] (Sirimanne & Hoffmann, 2019). Lower NO and soot emissions were observed during LeanShips: average decreases over the entire tested load and speed range of respectively 60% and 77%. The maximum methanol energy fraction (MEF) amounted to 70% and a relative increase in efficiency of 12% was recorded in dual-fuel operation [13] (Dierickx, Sileghem, & Verhelst, 2019). Given that a single point injection (SPI) strategy of methanol would require even less engine modifications and thus lower costs, both enabling an easier retrofit, methanol injectors were added to the Volvo Penta at a single point just behind the turbo-compressor. The details of the conversion are given in Section 2. It is expected that MPI has advantages in full load because of the evaporative cooling of methanol close to the engine, suppressing knock; and that SPI is advantageous in part load because of the lower cooling in that region (preventing e.g. misfires).

Although some dual-fuel fumigation literature exists, few attention is given to the position of the methanol injectors. Chen et al. have explicitly compared SPI with MPI [14] (Chen, et al., The impact of methanol injecting position on cylinder-to-cylinder variation in a diesel methanol dual fuel engine, 2017) with a focus on cylinder-to-cylinder variations. They have investigated two single point locations and it can be concluded that the distance from the single injection point to the cylinders and the intake air temperature at the injection point are important parameters to ensure a complete evaporation of methanol in the intake air flow. Injection too close to the cylinders can cause an incomplete evaporation and mixing resulting in more methanol entering in the more easily reachable cylinders. Further they concluded between the better SPI position of the two and MPI: that in both cases the cylinder-to-cylinder and cycle-to-cycle variations were similar, that NOx and CO were slightly lower in MPI mode, and that soot was slightly lower in SPI mode. They however did not investigate the impact of the methanol injection position on the maximum MEF, on engine retrofit practicalities and on efficiency. Other research papers can be split in two categories: those that have converted their engine with an MPI strategy and those that use SPI. These papers however do not give explicit attention to the particularities of the methanol injection position. A gap of knowledge is observed when one wants to take a decision on the most suitable methanol injection position for retrofitting diesel engines to dual-fuel operation.

Therefore, this paper has the goal to contribute to this gap: this research compares MPI and SPI in more detail and investigates the effects and consequences of the methanol injection position. In Section 2 the technical design requirements of MPI and SPI and the engine setup are described, and in Section 3 the research method. Sustainable dual-fuel methanol-diesel engines are characterized by the possibility to use a high share of methanol, and thus a high MEF, with high efficiency and with low emissions to meet the stringent IMO emission legislation. The experimental results with regard to maximum attainable MEF, efficiency and NO_x emissions are therefore given in Section 4. In Section 5 both methanol injection modes, MPI and SPI, are discussed from a point of view to bridge the results towards other engine retrofits.

2. Engine conversion to dual-fuel with methanol

2.1. Technical design requirements

When starting a conversion of a diesel engine to dual-fuel operation with methanol-diesel, an important design choice is where to install the methanol injectors. The impact of the injector’s position on the ease of installation and on the engine performance are of importance.

In MPI the injectors are installed closest to the engine and directed on the intake valves, meaning that this position has to be physically reachable. We have learned that engines with crossflow cylinder head, having the inlet on one side and the exhaust on the other side, are easier to convert than engines with a reverse-flow cylinder head, having inlet and exhaust on the same side, because the inlet in crossflow cylinder heads is typically more easily reachable. The engine used in this research (details see next Section) has a reverse-flow cylinder head and therefore challenges were encountered during the installation of the injectors: the intercooler needed a new position to enable space for the methanol low pressure fuel rail, resulting in adapted connections between the turbo-compressor and the intercooler, and between the intercooler and the intake manifold. The result of these adaptations are visualized on Fig. 1. The advantage of MPI is that an equal amount of methanol is injected close to the cylinder enabling to fully benefit the cooling effect of methanol which has a positive effect on engine performance [15] (Coulier & Verhelst, 2016). Because of the conversion challenges in MPI it is therefore questioned whether a single point injection strategy, which is easier to install and thus comes with a lower conversion cost, gives similar performance as MPI.

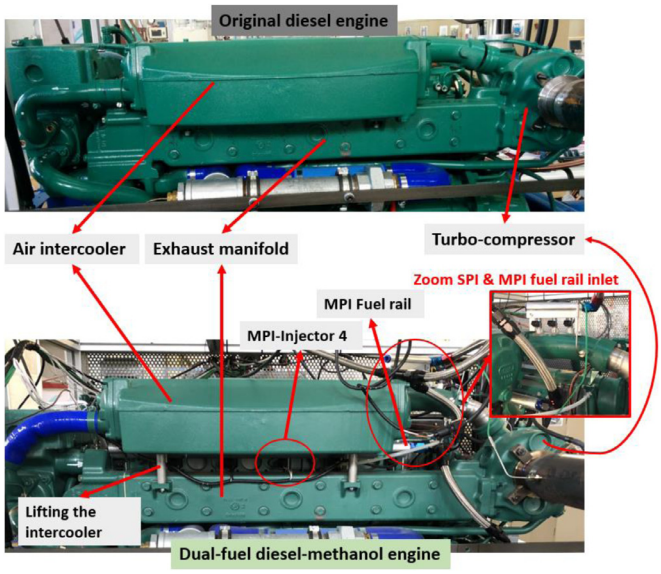

Fig. 1. Original diesel engine and converted engine to dual-fuel diesel-methanol operation.

A single point injection however comes along with other technical design requirements: (1) the mixing length after methanol injection has to ensure proper mixing before the intake manifold is reached, (2) condensation of methanol in the intake has to be avoided at all time meaning that the temperature has to be above its dew point, and (3) a proper distribution of the methanol-air mixture to each cylinder is required, which is influenced by the air pathway to the cylinders and thus by the shape of the intake.

The injector position was chosen just behind the turbo-compressor. In this point temperatures were high and greater than methanol's dew point (see further in next Section and on Fig. 4) and thus ensuring full evaporation of methanol. An implication of the above requirement (2) was that the intercooler had to be removed or bypassed in SPI operation: the intercooler would lead (as discussed in next Section) to condensation of methanol. In this research the intercooler operation was disabled, but in future research it should be tested whether controlling the intercooler's power would not give better results in some operating points. The methanol injection point in SPI mode was furthermore chosen to ensure the highest mixing length of the methanol air mixture before reaching the intake manifold. The Volvo Penta has an asymmetric intake manifold, as can be seen on Fig. 3, having an impact on requirement (3). The impact of this type of intake geometry will be discussed in Section 4.2.4.

2.2. Engine setup

The main characteristics of the test engine, a Volvo Penta D7C-B TA, are given in Table 1. To enable dual-fuel operation, new components and sensors were installed:

- A methanol fuel supply system: a pump, two filters, a pressure regulator (regulating the injection pressure at 5 bar), and nine methanol injectors (for MPI mode one at each cylinder, and for SPI mode three injectors behind the turbo-compressor were sufficient to reach the necessary methanol mass flow).
- Measurement sensors: mass flow sensors (diesel, methanol, air), temperature sensors (exhaust gases, intake air, and cooling water) and pressure sensors at cylinder number one (intake, exhaust and in-cylinder).

Table 1
Main specifications of the test engine.

Model	D7C-B TA
Aspiration	Turbocharged with air intercooler
Cylinders	6, in-line
Compression ratio	19
Bore x stroke	108 mm x 130 mm
Displacement volume	7,15 l
Diesel injection system	Cam-driven Single Injection Pumps
Diesel injection pressure	1200 bar
Maximum torque / speed / bmep	904 Nm / 1500 rpm / 15.9 bar
Rated power / speed / bmep	195 kW / 2300 rpm / 14.2 bar

Table 2
Details of the methanol supply and measurement system.

Methanol supply system	
Injectors	Magneti Marelli IWPR02
Pump & filters	Fuelab pump (41401c) & filters (60 & 75 µ)
ECU	Motec M800
Measurement equipment	
Mass flow	Bronkhorst M15 (diesel & meoh) & F (air)
Pressure	Keller M5HB (low p) & Kistler 6045B (high p)
Temperature	K-type (high T) & J-type (low T)
Load	Logicontrol H3
Data acquisition	NI DAQ 9205, 9213, 9215, 9401
Emissions	MAIHAK Unor 610

- An engine control unit (ECU) to control the methanol injection timing and a data-acquisition system to acquire and process all measurement data.

All these components and sensors were installed separately from the original Volvo Penta control system. This means that the original diesel supply and mechanical engine control system were not changed. The diesel injection amount remained to be controlled by the original engine's governor and a manual speed rod controlled by the engine operator. Table 2 gives the details of the new components and sensors.

Fig. 2 shows a schematic view of the engine setup with the most important components. Fig. 3 zooms in on the two different methanol injection positions: (1) in the intake manifold directed to the intake valves (MPI), and (2) in the pipe connecting the turbocharger and the intake manifold (SPI). The single point was chosen such that the distance to the cylinders was longest to ensure proper methanol-air mixing. There are three methanol injectors in SPI mode located behind the turbo-compressor, which are positioned with an angle of 30° versus the flow direction looking in the horizontal plane. The distance in the flow direction between the first and third injector is 90 mm; the distance between the intake temperature sensor and the first and third injector respectively are 415 mm and 325 mm. We have assumed that this distance ensures complete evaporation with air before the intake temperature measurement point. Note further that the intake manifold is asymmetric, which is an important characteristic of the engine because it has an influence on the engine performance as will be discussed in Section 4. On Figs. 2 and 3a three way valve is shown with the functionality to decide whether the intercooler (IC) is bypassed or not. In reality this functionality is present on the engine setup but manually realized without an actual three way valve: in SPI mode the IC is dismantled and replaced by a tube connecting the turbocharger and the intake air manifold.

The reason for removing the IC in SPI mode is that the IC's cooling power cannot be altered – which is necessary in SPI mode: given methanol's high heat of evaporation, injection of methanol results in a considerable cooling of the intake air. Adding the IC's cooling power would lead to condensation in the IC. This is illustrated in Fig. 4 that shows temperatures at 1500 rpm for two

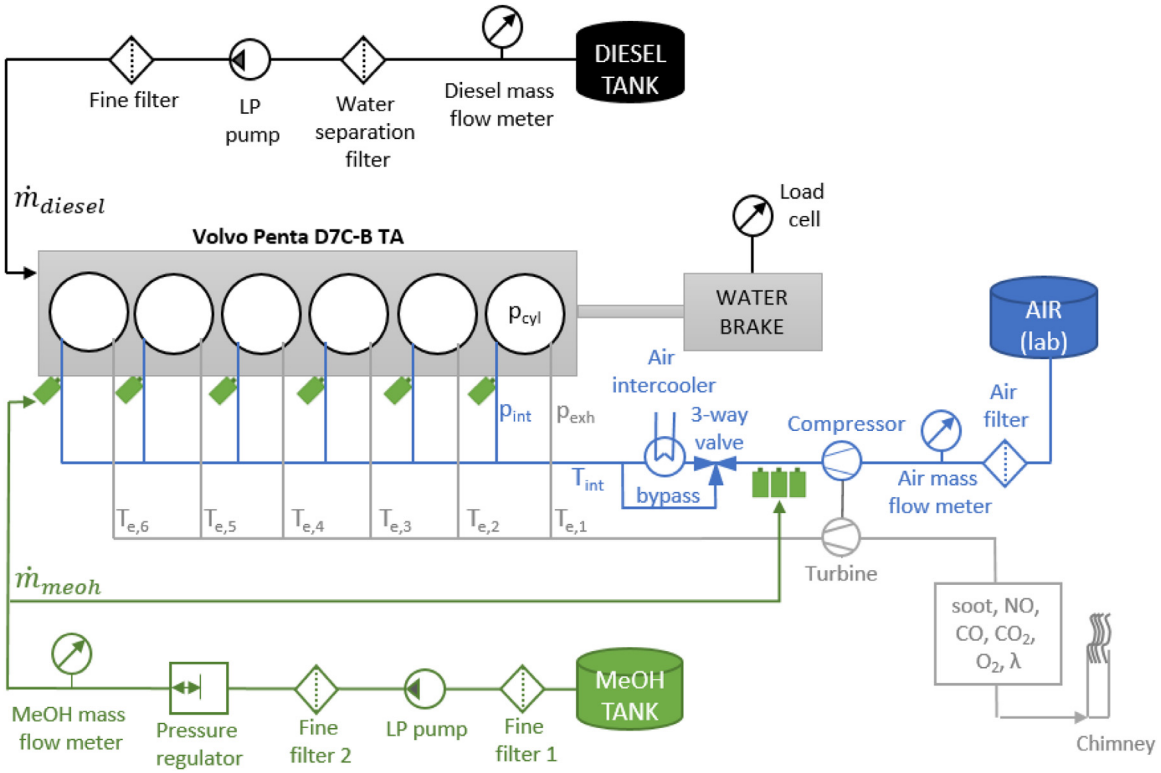

Fig. 2. Schematic view of the engine setup.

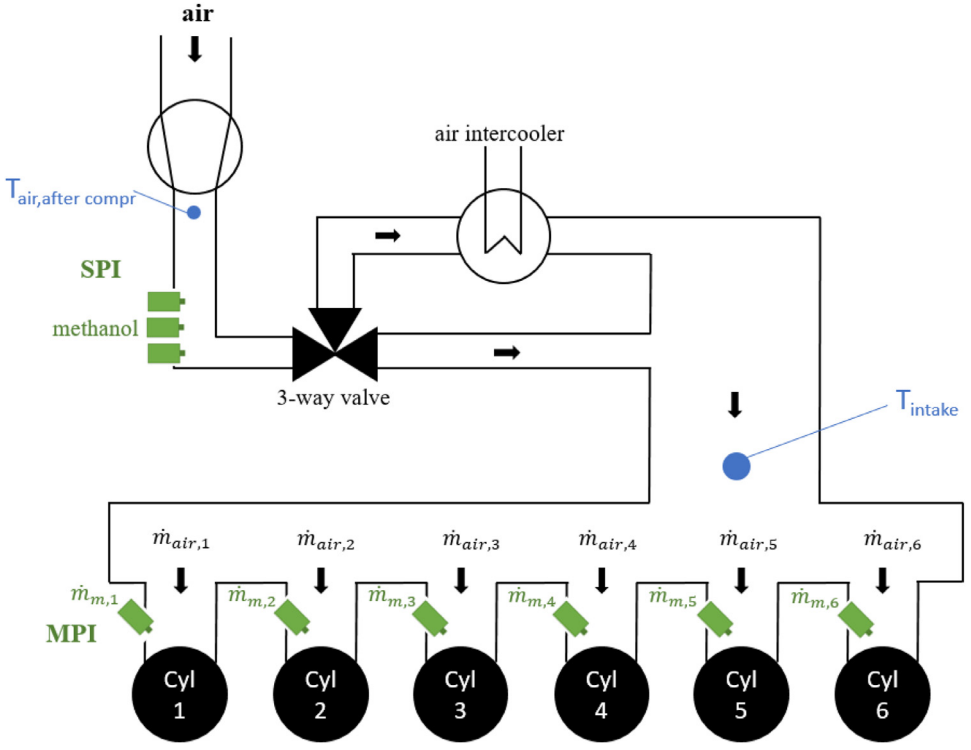

Fig. 3. Detailed schematic of the intake air manifold and the methanol injector positions.

loads, before and after methanol injection, as a function of MEF. The temperature before methanol injection equals the temperature after the turbo-compressor, as shown in Fig. 3. The temperature after methanol injection is a calculated temperature, assuming that methanol takes all energy to evaporate from the air (the most extreme case). As can be seen, very low temperatures occur at high MEF. To prevent condensation in the IC, the IC was therefore removed in SPI mode. A consequence of not using the IC in SPI mode is that the intake air temperatures will be higher than in MPI mode, as will be discussed in Section 4.

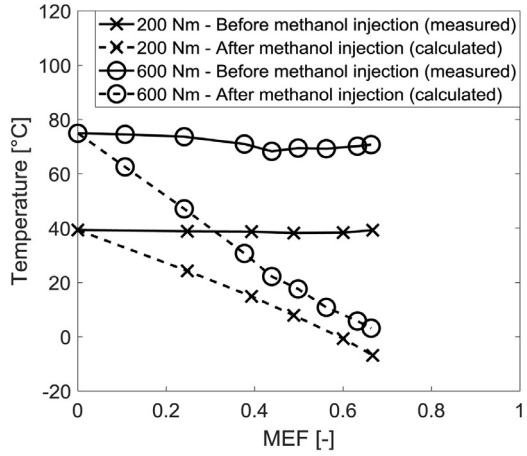

Fig. 4. Intake temperatures before and after methanol single point injection as a function of MEF.

3. Methodology

3.1. Definitions

Dual-fuel operation is characterized by the combustion of two fuels. To define the amount of each fuel used, different definitions are used. The four main encountered definitions are: Methanol Energy Fraction (MEF), Diesel Substitution Ratio (DSR), Methanol Mass Fraction (MMF), and Replacement Ratio (RR). The equations are as follows:

$$MEF = \frac{\dot{m}_m \cdot LHV_m}{\dot{m}_m \cdot LHV_m + \dot{m}_d \cdot LHV_d}$$

$$DSR = \frac{\dot{m}_{d,DO} - \dot{m}_{d,DF}}{\dot{m}_{d,DO}}$$

$$MMF = \frac{\dot{m}_m}{\dot{m}_m + \dot{m}_d}$$

$$RR = \frac{\dot{m}_m}{\dot{m}_{d,DO} - \dot{m}_{d,DF}}$$

With the subscript m and d respectively denoting methanol and diesel; the subscript DO and DF respectively denoting diesel-only operation or dual-fuel operation; $\dot{m}$ standing for mass flow and LHV for lower heating value. Each definition gives different information. MEF denotes the amount of energy in the cylinder that comes from methanol versus the total available fuel energy. The MMF is similar but compares the mass of methanol to the total fuel mass. The DSR indicates how much of the diesel is being replaced compared to DO. The RR gives direct information on the efficiency of the diesel replacement. Given that in stoichiometric operation one needs 2.14 times more methanol mass than diesel mass to reach the same fuel energy in the cylinder, it follows that when RR is higher than 2.14 the efficiency is decreasing, and vice versa. In this research the MEF is used to characterize the amount of methanol as it indicates the methanol energy used in each operating point. Because MEF gives no information on the amount of diesel and thus greenhouse gasses that can be saved (when using renewable methanol), the relation between MEF and DSR is shown in Section 4.2.2.

The in-cylinder pressure data used in Section 4 was based on the best-fit method. First the average in-cylinder pressure over 100 cycles is calculated and this pressure is compared with the measured pressures in each cycle. The pressure profile that is closest to the average profile is taken for analysis purposes. The heat release rate (HRR) is calculated based on the first law of thermodynamics:

$$\frac{dQ}{d\theta} = \frac{\gamma}{\gamma - 1} \cdot P \cdot \frac{dV}{d\theta} + \frac{1}{\gamma - 1} \cdot V \cdot \frac{dP}{d\theta}$$

With Q the heat release, θ the crank angle, P the in-cylinder pressure, and V the instantaneous volume of the combustion chamber. Gamma was fixed at 1.35. Based on the HRR, the CA10, CA50, CA90 and the combustion duration (CA10-CA90) were calculated. The start of diesel injection (SOI) is not known, but as the engine has individual pumps per cylinder driven by the camshaft (pump-line-nozzle system), it is assumed that the SOI is constant at a certain engine speed independent of the diesel injection amount. The average in-cylinder temperature was calculated based on the ideal gas law ($p \cdot V = m \cdot R \cdot T$, with m assumed to be equal to the total cylinder mass (air, methanol and diesel); the specific gas constant, R, calculated based the exhaust gas composition; and p, V, T respectively the instantaneous in-cylinder pressure, volume and temperature), and is used in the next Section as an indication of the in-cylinder temperature. The specific emissions were calculated based on the guidelines of IMO in Marpol/CONF.3/34 [16] (IMO, 1997).

The measurement uncertainty on the different engine performance parameters, $\delta_q(x_1,x_2,\ldots,x_n)$, was calculated by using Taylor's error equation [17] (Taylor, 1997):

$$\delta q(x_1, x_2, \ldots, x_n) = \sqrt{\left(\frac{\partial q}{\partial x_1} \cdot \delta x_1\right)^2 + \left(\frac{\partial q}{\partial x_2} \cdot \delta x_2\right)^2 + \ldots + \left(\frac{\partial q}{\partial x_n} \cdot \delta x_n\right)^2}$$

in which x_1, x_2, ..., x_n and δx_1, δx_2, ..., δx_n are respectively the measured values by which $q(x_1,x_2,\ldots,x_n)$ is calculated and the uncertainties on the measured values. Applied to λ, BTE and $NO_{(2)(x)}$, the engine performance parameters discussed in Section 4, this gives:

$$\lambda_m = \frac{\frac{\dot{m}_a}{\dot{m}_m}}{L_{s,m}}$$

$$\lambda_{d-m} = \frac{\frac{\dot{m}_a}{\dot{m}_m + \dot{m}_d}}{MMF \cdot L_{s,m} + (1 - MMF) \cdot L_{s,d}}$$

$$\delta\lambda_m{}^2 = \left(\frac{1}{\dot{m}_m \cdot L_{s,m}} \cdot \delta\dot{m}_a\right)^2 + \left(\frac{\dot{m}_a}{\dot{m}_m^2 \cdot L_{s,m}} \cdot \delta\dot{m}_m\right)^2$$

$$\delta\lambda_{d-m}{}^2 = \left(\frac{1}{(\dot{m}_m + \dot{m}_d) \cdot \left(MMF \cdot L_{s,m} + (1 - MMF) \cdot L_{s,d}\right)}\right)^2 \cdot \left(\delta\dot{m}_a^2 + \dot{m}_a^2 \cdot \left(\delta\dot{m}_m^2 + \delta\dot{m}_d^2 + \frac{\left(L_{s,m} - L_{s,d}\right)^2}{\left(MMF \cdot L_{s,m} + (1 - MMF) \cdot L_{s,d}\right)^2} \cdot \delta MMF^2\right)\right)$$

$$BTE = \frac{P_e}{\dot{m}_m \cdot H_{u,m} + \dot{m}_d \cdot H_{u,d}}$$

$$\delta BTE^2 = \left(\frac{1}{\dot{m}_m \cdot H_{u,m} + \dot{m}_d \cdot H_{u,d}}\right)^2 \cdot \left(\delta P_e^2 + \left(\frac{P_e \cdot H_{u,m}}{\dot{m}_m \cdot H_{u,m} + \dot{m}_d \cdot H_{u,d}}\right)^2 \cdot \left(\delta\dot{m}_a^2 + \delta\dot{m}_d^2\right)\right)$$

$$NO_{(2)(x)} = \frac{NO'_{(2)(x)}}{P_e}$$

$$\delta NO_{(2)(x)}{}^2 = \left(\frac{1}{P_e} \cdot \delta NO'_{(2)(x)}\right)^2 + \left(\frac{1}{P_e} \cdot \delta P_e\right)^2$$

Table 3
Tested load and speed area.

1000 rpm	3.51; 7.03 bar bmep
1500 rpm	3.51; 7.03; 10.55; 12.31 bar bmep
2000 rpm	3.51; 7.03; 10.55 bar bmep

with the stoichiometric air fuel ratio of methanol ($L_{s,m}$) and diesel ($L_{s,d}$) respectively 6.5 kg air/kg methanol and 13.92 kg air/kg diesel; subscript D-m and a denoting respectively diesel-methanol and air; P_e the brake thermal power equal to $2 \cdot \pi \cdot T_e \cdot n$ with T_e and n respectively the brake torque and the engine speed; H_u the lower heating value; $NO_{(2)(x)}$ and $NO'_{(2)(x)}$ the $NO/NO_2/NO_x$ emissions in respectively g/kWh and g/h. The uncertainties of the individual measurements are: $\delta\dot{m}_m = \delta\dot{m}_d = 2\% \cdot reading\ kg/h$, $\delta\dot{m}_a = 0.5\% \cdot reading + 1.225\ kg/h$, $\delta T_e = 18.7\ Nm$, $\delta n = 5\ rpm$, and $\delta NO_{(2)(x)} = 1\% \cdot reading + 15\ ppm$.3.2 Measurement matrix and test procedure

In Table 3, the tested load and speed area is given: in both MPI and SPI mode three different engine speeds were tested with different loads at each speed. In the analysis in Section 4 often only the results at 1500 rpm are shown in order to not overload the figures.

The measurement campaign had the objective to compare MPI and SPI mode for three different engine performance parameters: maximum allowable MEF, efficiency and NO_x emissions. At each load point first the modus operandus was selected (MPI or SPI) followed by setting up the right speed and load in diesel-only mode. Once the data was acquired in the DO point, the methanol fraction was increased by the engine operator (with the ECU) in small steps and the diesel fraction decreased (with the manual speed rod controlling the original engine's governor) to maintain the same speed and load, and this repeatedly until the maximum MEF was reached. At some intermediary points between DO and the limit of diesel substitution (typically in steps of 10% MEF), all measurement data was acquired.

As a start, the criteria to determine the maximum MEF developed in [18] (Wang, Wei, Pan, & Yao, 2015) were used. Wang et al. defined four boundary events: (1) partial burn, (2) misfire, (3) roar combustion and (4) knock. Partial burn was defined as introducing more methanol without an increase of output torque but with an excess of unburned methanol emitted to the exhaust. Misfire was detected via a combustion analyzer, and roar combustion and knock were detected respectively by limiting the peak pressure rise rate (PPRR) at 15 bar/ °CA and the peak cylinder pressure (PCP) at 150 bar (mechanical design limit of the engine). The limit of the PPRR was set to limit engine noise, and the PCP to protect the engine from high mechanical stress. New criteria had to be developed, however, as the criteria of Wang et al. were not all applicable on the Volvo Penta. This will be returned to in Section 4.2.

3.3. Interpretation of results

In next Section when discussing the results, SPI will implicitly imply no intercooler, unless differently stated, and MPI will imply with intercooler. This in order to avoid repetition of engine setup differences between both modes. Further, as mentioned above only in-cylinder pressure was measured in cylinder one, and based on this measurement HRR and in-cylinder temperature was calculated using the equations in Section 3.1. This will not be mentioned when discussing on in-cylinder pressure and temperature, and HRR, unless relevant for the results.

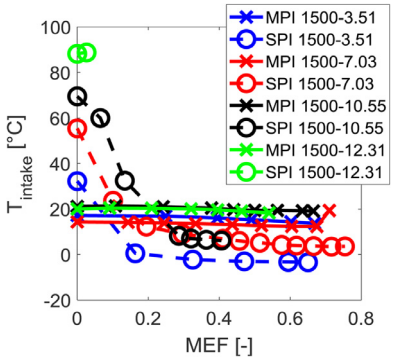

Fig. 5. Intake charge temperature in MPI and SPI mode at 1500 rpm.

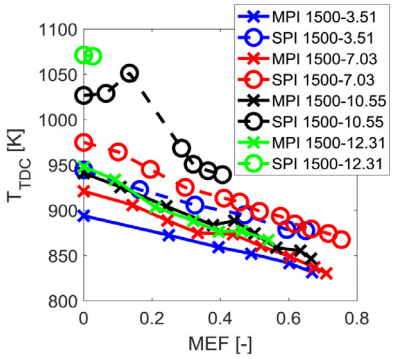

Fig. 6. Temperature at TDC in MPI and SPI mode at 1500 rpm.

4. Results

4.1. Intake temperatures in MPI and SPI

We first take a look at the intake temperature and the temperature at top dead centre (TDC) in the two methanol injection modes, as these will explain observed differences in next Sections. The temperature differences in both modes are caused by the intercooler that had to be removed in SPI mode to prevent methanol condensation after injection. Fig. 5 shows the intake temperatures at 1500 rpm for different loads. Note the difference in running the engine between both modes as defined in Fig. 3: this means that in SPI mode the temperature shown is that of the air-methanol mixture, and in MPI mode this is the air temperature after the IC as methanol is only injected after this measurement point. In SPI mode negative intake charge temperatures were measured at 3.51 bar bmep for MEFs higher than 16%; and temperatures below 10 °C at 7.03 and 10.55 bar bmep for MEFs higher than 19%. In SPI-DO the air temperatures are high (32–88 °C) as no IC is present. In MPI mode the intake temperature is rather constant as a function of MEF and lies between 12 °C and 21 °C, depending on the load.

The resulting temperature at TDC is calculated and shown in Fig. 6 in MPI and SPI mode. It can be seen that the temperature at TDC decreases as a function of MEF, which is due to the cooling effect of methanol. The temperatures at TDC are lower for MPI than for SPI, although the inverse was true for T_{intake}. This is due to the multiple point methanol injection that further cools the intake air. Note the increase in T_{TDC} in SPI at 10.55 bar bmep with 14% MEF. In this point pre-ignition of the methanol-air mixture occurs. This phenomenon will be further discussed in Section 4.2.

4.2. Methanol energy fraction

4.2.1. Maximum methanol energy fraction

One of the most essential parameters in a dual-fuel methanol-diesel engine is the maximum methanol energy fraction. This is because it is a measure for the sustainability that can be reached. If renewable methanol is used and if the maximum MEF is high, then more of the fossil diesel can be replaced. A more direct parameter is the DSR as it directly indicates how much diesel can be substituted and thus how much the global warming potential is reduced. In this work the MEF is used as it indicates how much of the total fuel energy is coming from methanol. To make the link with DSR however, the relation between MEF and DSR is visualized in Section 4.2.2.

To reach the maximum MEF in MPI and SPI mode, we started from the criteria described in Section 2.2. The criteria were verified at each tested operating point, however not all criteria appeared to be useable. A decreasing efficiency was observed in some low load points when introducing more methanol, pointing to partial burn, though this event could not be defined with certitude as no methanol exhaust gas measuring device is present on the setup. Secondly, as the engine setup has only one in-cylinder pressure sensor (in cylinder one), misfire could not be detected in all cylinders. The peak pressure rise rate (PPRR) limit could also not be used to detect roar combustion as the maximum PPRR measured over the entire tested load range was only 9.3 bar/°CA (at 1000 rpm and 7.03 bar bmep with 58% MEF). Finally, the maximum measured PCP, used as a knock detection, was only 110 bar (at 1500 rpm and 12.3 bar bmep with 54% MEF), and thus not exceeding the maximum allowable in-cylinder pressure of the Volvo Penta being 140 bar.

Therefore other criteria were developed for detecting the diesel substitution limits. Misfire was detected by a sudden and continuous fall of one or more cylinder exhaust temperatures. Partial burn was defined as a significant decrease of one (or more) cylinder exhaust temperature(s). The difference with misfire is that in partial burn a new exhaust temperature equilibrium was found. Partial burn finally resulted in misfire when further increasing the methanol fraction. Knock is defined as the auto-ignition of the methanol-air mixture after diesel ignition. This event was detected by ear, based on the engine's sound signature. It is a suddenly changing engine sound – best described as a metal pinging sound – that undoubtedly results in the conclusion that knock is occurring. Another phenomenon was included as a diesel substitution limiting event, being pre-ignition of the methanol-air mixture before diesel ignition. To detect pre-ignition the in-cylinder pressure sensor was used, and consequently only pre-ignition in cylinder 1 could be detected. Exceedingly high exhaust temperatures were also added to the list of criteria to detect a substitution boundary, pointing to a very late combustion. This condition was met when the exceptional exhaust temperature was 15% more than the average exhaust temperature and points

Using these criteria, the maximum MEF values and diesel substitution limiting events in Figs. 7 and 8 were obtained in respectively MPI and SPI mode. The maximum measured MEF of 84% was observed in SPI mode at 2000 rpm and a bmep of 7.03 bar. At this point the DSR amounts to 79%, which means that taking only the engine into consideration, a CO_2 emission reduction of 79% can be reached with renewable methanol. In MPI mode the maximum MEF amounted to 80%. It can be seen that in 6 of the 9 tested load points a higher maximum MEF was obtained in MPI mode. The average maximum MEF in MPI mode amounted to 67% and in SPI mode to 45%.

The diesel substitution limiting events in MPI mode are partial burn, misfire and knock. At low engine speed no knock was observed. Misfire tended to be independent of engine speed and load. Partial burn on the other hand has only occurred at low engine speed. It can be furthermore seen on Fig. 7 that the maximum MEFs are quite similar for the two lowest loads (3.51 and 7.03 bar bmep) as a function of engine speed.

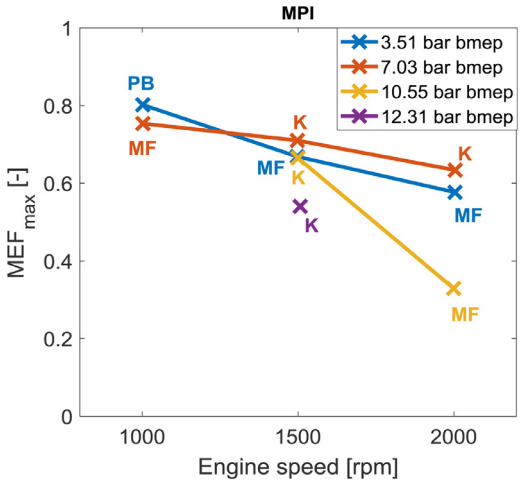

Fig. 7. Maximum methanol energy fractions as a function of engine speed. Abbreviations: PB = Partial Burn, MF = Misfire, K = Knock.

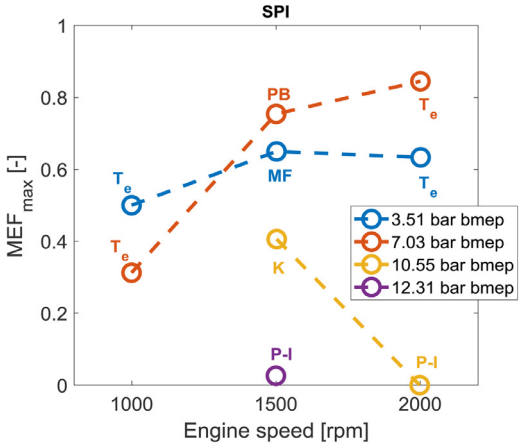

Fig. 8. Maximum MEF in SPI mode as a function of engine speed. Abbreviations: PB = Partial Burn, MF = Misfire, K = Knock, T_e = exceedingly high exhaust temperatures, P-I = Pre-Ignition.

In SPI mode two additional substitution limits were observed: pre-ignition and exceedingly high exhaust temperatures. The maximum MEFs are more spread than in MPI mode, and in case of pre-ignition only a very low MEF could be reached. These additional substitution limits could be linked with the effect of the intercooler that is not present in SPI mode, resulting in higher intake temperatures, and with the asymmetric intake manifold resulting in cylinder-to-cylinder variations. In the next Sections these observations are further analyzed.

4.2.2. Relation between MEF and respectively DSR and λ

From a sustainability point of view DSR is more interesting because it gives direct information on the amount of diesel that has been replaced. Assuming fossil diesel is replaced by renewable methanol, one can say that the amount of greenhouse gases that are saved compared to DO is equal to the value of DSR. If DSR amounts for example to 42%, then 42% of fossil diesel is replaced by renewable methanol and thus 42% greenhouse gas emissions are avoided. Fig. 9 shows the relation between DSR and MEF at 1500 rpm in MPI and SPI mode. The line DSR = MEF is shown to give an indication of whether DSR is higher or lower than a certain

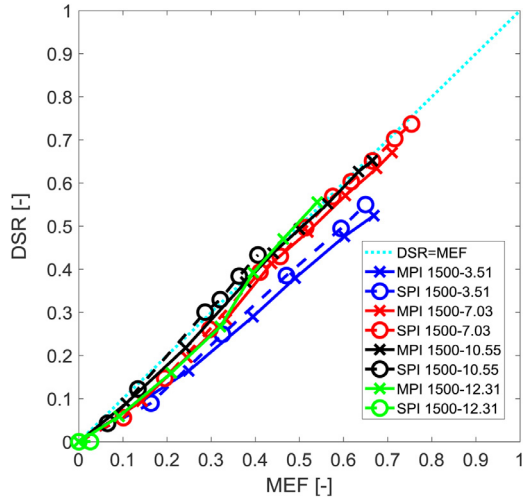

Fig. 9. Relation between MEF and DSR at 1500 rpm for MPI and SPI mode.

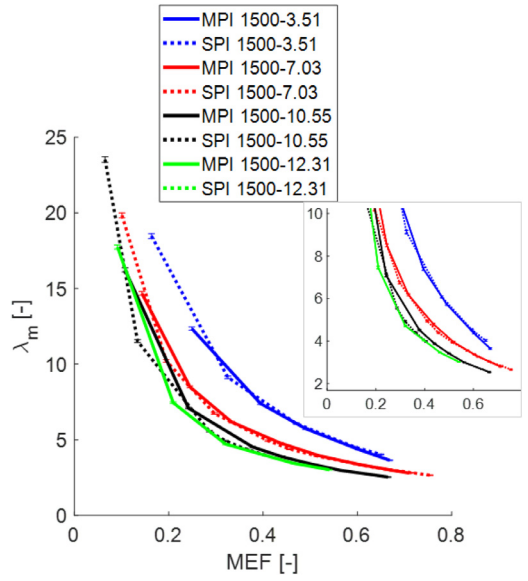

Fig. 10. λ_m as a function of MEF at 1500 rpm.

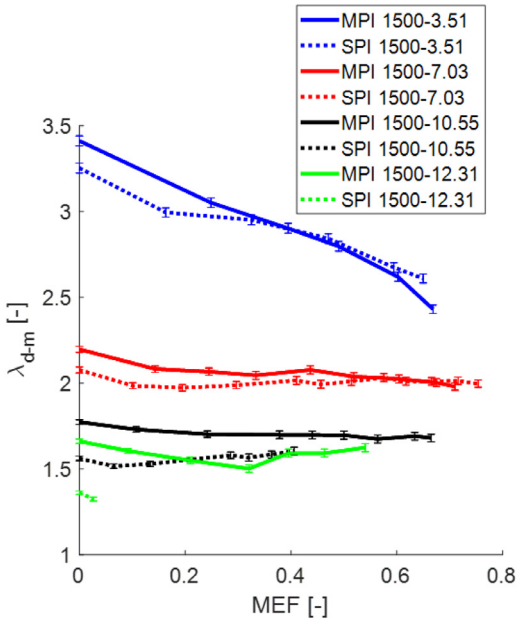

Fig. 11. $\lambda_{d\text{-}m}$ as a function of MEF at 1500 rpm.

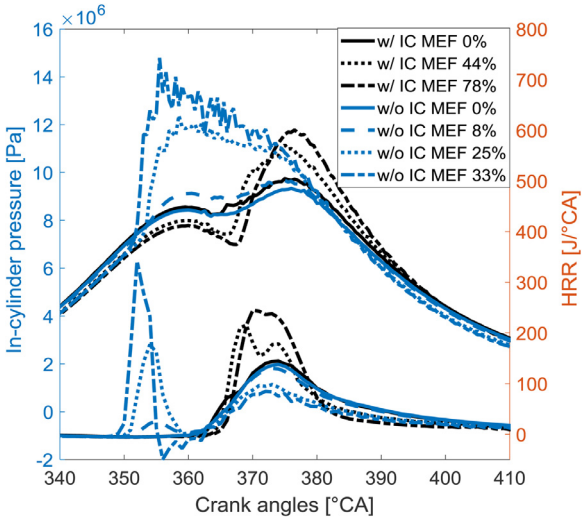

Fig. 12. Pressure and HRR in MPI mode with and without intercooler at 1500 rpm and 12.31 bar.

MEF value. It can be seen that only some SPI and MPI points (10.55 and 12.31 bar bmep) have for a certain MEF a higher DSR. The highest DSR is reached in SPI mode at 7.03 bar bmep and amounts to 74%.

The maximum MEF and DSR are dependent on several conditions and also depend on engine specific characteristics, such geometry and presence of an intercooler (as is subject in next Section). Figs. 10 and 11 therefore show respectively λ_m and $\lambda_{d\text{-}m}$, as defined in Section 3.1, which are more engine independent parameters. The lower and upper flammability limits of methanol in air (at 20 °C and atmospheric pressure) are respectively 6.7 and 36 vol%, which do translate in a λ of 1.81 and 0.23 [2] (Verhelst, Turner, Sileghem, & Vancoillie, 2019). It should be noted that these limits expand with increasing temperature and pressure, and thus bigger under high temperature and pressure engine conditions. It can be seen though that λ_m stays well above the lean flammability limit of 1.81. The lowest λ_m amounts to 2.53. For MEFs between 0 and 0.25, λ_m varies between 25 and 7, and for MEFs between 0.25 and 0.75, λ_m varies between 7 and 2.53. On Fig. 11 $\lambda_{d\text{-}m}$ is shown. It can be seen that at low load $\lambda_{d\text{-}m}$ enriches with increasing MEF, and that higher load $\lambda_{d\text{-}m}$ is more constant as a function of MEF.

4.2.3. Effect of intercooler on pre-ignition

Pre-ignition of methanol limits the maximum MEF in SPI, and therefore influence factors on this phenomenon are investigated in this Section. As pre-ignition was only observed in SPI mode and not in MPI mode, it is questioned what the effect of the air intercooler (IC) and thus of the intake charge temperature on pre-ignition is. To investigate this, additional MPI tests were performed with and without intercooler at 1500 rpm for 10.55 and 12.31 bar bmep. Two questions arise: (1) what is the difference between MPI with and without intercooler, and (2) is there a difference between MPI and SPI when both are operated without intercooler.

To address the first question, Fig. 12 shows the HRR and in-cylinder pressure in MPI at 1500 rpm and 12.31 bar bmep, with and without intercooler. It can be seen that with intercooler the maximum MEF that can be reached amounts to 78%. Without intercooler this is only 4%. At MEFs more than 4% pre-ignition occurs and the amount of methanol that pre-ignites only increases in significance with increasing MEF. At an MEF of 33% there is a

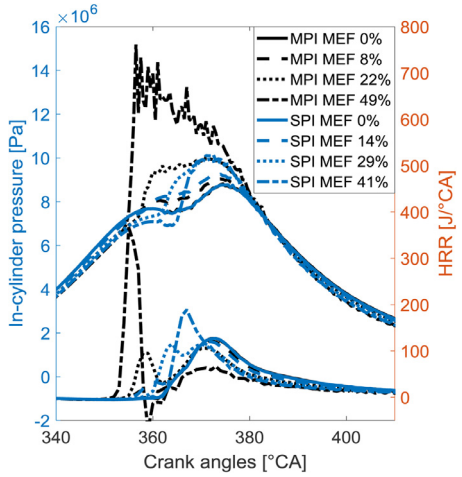

Fig. 13. Pressure and HRR at 1500 rpm and 10.55 bar bmep without intercooler in MPI and SPI.

large heat release before TDC and a smaller heat release after TDC which indicates that the methanol premixed combustion and the diesel combustion occur mainly independently from each other. In the case of pre-ignition with 25% and especially 33% MEF there are high pressure oscillations around TDC. The intake temperatures as defined by Fig. 4 are between 14 and 15 °C with intercooler and between 79 and 85 °C without intercooler. The intercooler thus cools the air with about 70 °C. As a consequence, the temperatures during the compression stroke are higher without intercooler, giving rise to pre-ignition. This points to a relation between intake charge temperature and pre-ignition, however it cannot be determined whether the pre-ignition is caused by a hot spot (i.e. is due to surface ignition) or by auto-ignition of the methanol-air mixture.

To address the second question, the difference between MPI and SPI, both without intercooler, Fig. 13 shows the HRR and the in-cylinder pressure at 1500 rpm and 10.55 bar bmep without IC for both MPI and SPI. The intake temperatures in SPI are shown on Fig. 5, while in MPI they lie between 58 and 71 °C. It can be seen that pre-ignition now occurs in both methanol injection modes. However, in SPI pre-ignition disappears with increasing MEF. With 41% MEF there is no pre-ignition while at MEFs of 14% and 29% there is. This can be linked to the charge cooling of methanol preventing pre-ignition: the intake temperatures decrease in SPI and amount for the MEFs of 0%, 14%, 29%, 41% to respectively 70 °C, 32 °C, 8 °C and 6 °C. The corresponding average in-cylinder temperatures at inlet valve closing (IVC) are respectively 146 °C, 133 °C, 120 °C and 117 °C. In MPI the amount of methanol that pre-ignites increases with increasing MEF and pre-ignition starts at earlier crank angles. It should be noted that pre-ignition only disappeared in SPI at 1500 rpm and 10.55 bar bmep. At 1500 rpm and 12.31 bar bmep and at 2000 rpm and 10.55 bar bmep the amount of methanol that pre-ignited before TDC only increased when further increasing MEF (finally resulting in knock).

In case of MPI, the methanol injectors are directed at the back of the intake valves, to make use of the heat of the valves to aid with fuel evaporation. This seems to work too well, in the sense that the heat of vaporization indeed seems to come primarily from the intake valve and hence the intake air is less cooled compared to the SPI case. An indication for this reasoning is the low cooling and spread in the average in-cylinder temperatures at IVC: the intake temperatures in MPI and the temperatures at IVC amount for the MEFs of 0%, 8%, 22% and 49% to respectively 70 °C, 70 °C, 68 °C and 60 °C and to respectively 148 °C, 141 °C, 138 °C and 138 °C. At an MEF of 49% there is thus no real decrease in average temperature at IVC compared to T_{intake} with increasing MEF, while in SPI the intake air temperature decreases from 70 °C to 6 °C when going from 0% MEF to 41% MEF. As this indication is based on average in-cylinder temperatures, this hypothesis should be investigated further because it ignores spatial temperature differences.

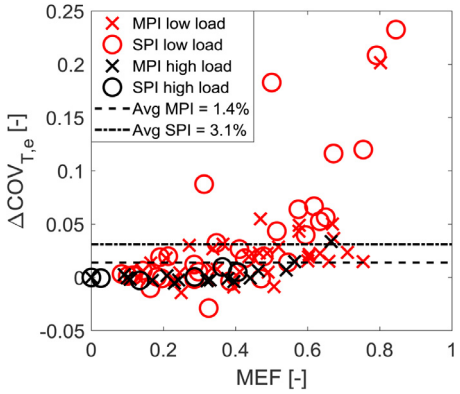

Fig. 14. $\Delta COV_{T,e}$ in MPI and SPI mode as a function of MEF and split for high and low load.

4.2.4. Effect of asymmetric intake manifold on maximum MEF

Given that the maximum MEFs were observed to be more spread out in SPI mode, it is questioned whether there is a link with cylinder-to-cylinder variations. As the Volvo Penta has an asymmetric intake air manifold (see Fig. 3), it is assumed that in SPI mode at high intake mixture velocities, methanol droplets are more keen to follow the easiest path. This would result in higher methanol quantities in cylinder 4, 5 and 6. The lower the intake manifold temperatures, the higher the probability that not all methanol is fully vaporized.

Since there is only one in-cylinder pressure sensor, the cylinder-to-cylinder variations cannot be quantified via the coefficient of variation (COV) of imep as in [19] (Chen, Yao, & Yao, The impact of methanol injecting position on cylinder-to-cylinder variations in a diesel methanol dual fuel engine, 2017). The only measurement at each cylinder on the test engine are of the exhaust temperatures. These temperature sensors are positioned just behind the exhaust valve and in front of the exhaust collector so there is little interference with exhaust gases from adjacent cylinders. The COV of the exhaust temperatures (in °C) has been calculated via:

$$COV_{T,e} = \frac{\sigma_{T_e}}{\mu_{T_e}} = \frac{\sqrt{\frac{\sum_{i=1}^{6}\left(T_{e,i}-T_{e,avg}\right)^2}{6}}}{\frac{\sum_{i=1}^{6} T_{e,i}}{6}}$$

In the following, $COV_{T,e,DO}$ is defined as the COV of the exhaust temperatures in diesel-only mode, and $COV_{T,e,DF}$ in dual-fuel mode at a certain MEF. To eliminate the variations between the exhaust temperatures in DO operation, the difference in COV between DF and DO operation, $\Delta COV_{T,e}$, is calculated in each load point:

$$\Delta COV_{T,e} = COV_{T,e,DF} - COV_{T,e,DO}$$

In Fig. 14 $\Delta COV_{T,e}$ is shown. The average $\Delta COV_{T,e}$ in MPI mode amounts to 1.4% and in SPI mode to 3.1%. The standard deviation in MPI mode amounts to 3.0% and in SPI mode to 5.7%. At high load the average $\Delta COV_{T,e}$ is 0.2% for both MPI and SPI, and at low load 2.0% and 3.7% for respectively MPI and SPI. Given the assumption that $\Delta COV_{T,e}$ gives an indication of the cylinder-to-cylinder variations, it can be deduced from this analysis that at low load the cylinder-to-cylinder variations are higher in SPI than in MPI, and that they are similar at high load. The higher spread in maximum

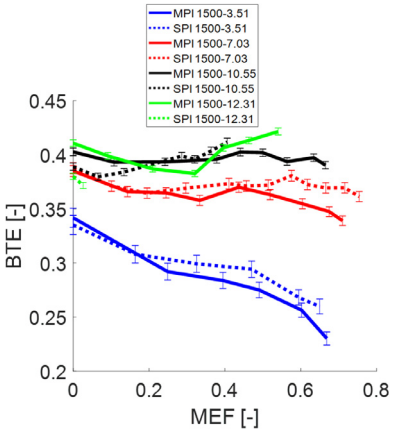

Fig. 15. Brake thermal efficiency as a function of MEF at 1500 rpm.

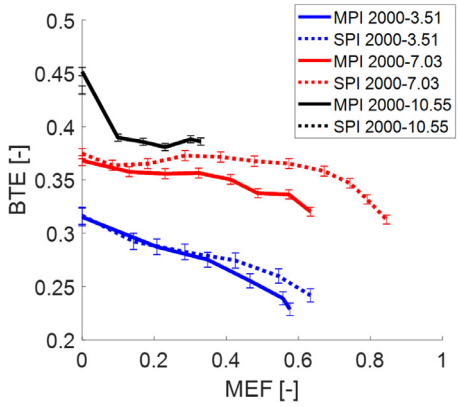

Fig. 16. Brake thermal efficiency as a function of MEF at 2000 rpm.

MEFs can thus reasonably be attributed to the higher cylinder-to-cylinder variations in SPI mode.

4.3. Efficiency

From literature it can be concluded that as a rule of thumb the brake thermal efficiency (BTE) decreases compared to DO with increasing MEF at low loads, and increases at high loads [15] (Coulier & Verhelst, 2016). At low loads this is ascribed to (1) the longer ignition delay (and thus retarded combustion), and (2) the lower burning velocity resulting from a leaner and colder mixture. At high loads, a higher BTE results from a faster and more isochoric combustion, caused by more fuel being burned in the premixed phase and by the higher flame speed of the richer methanol-air mixtures.

On Fig. 15 the BTE is shown for different loads at 1500 rpm. It can be seen that the results for low loads are in line with literature. At high loads the MPI and SPI measurements show rather a constant efficiency instead of an increasing efficiency with increasing MEF. It can be further seen that there is hardly any difference between MPI and SPI in efficiency, when taking into account the error bars, except at 7.03 bar bmep where at high MEFs the efficiency is higher in SPI mode.

In Fig. 16 the BTE is shown for different loads at 2000 rpm. It can be seen that at the lower loads of 3.51 and 7.03 bar bmep, the efficiency is higher in SPI mode for high MEFs. The most significant increase in BTE occurs at 2000 rpm and 7.03 bar with 60% MEF: a relative increase of 8.6% (from 33.6% to 36.5%). The reason for that is an earlier combustion phasing ($CA50_{MPI}$ = 18 °CA_{ATDC} while $CA50_{SPI}$ = 13 °CA_{ATDC}) and a slightly more isochoric combustion ($CA10–90_{MPI}$ = 39 °CA_{ATDC} while $CA10–90_{SPI}$ = 37 °CA_{ATDC}) in SPI than in MPI. The in-cylinder pressure and HRR in this load point are visualized in Fig. 17. In both modes lambda is equal (2.15) but the intake air mass decreases from 628 kg/h to 575 kg/h going from MPI to SPI. The average in-cylinder temperature at TDC in MPI mode is 907 K while in SPI mode this is 990 K. This higher temperature results in an earlier start of combustion and thus a combustion closer to TDC and a higher efficiency.

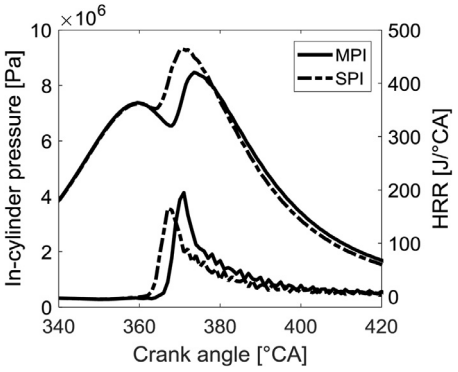

Fig. 17. Pressure and HRR in MPI and SPI at 2000 rpm and 7.01 bar bmep with 60% MEF.

4.4. Oxides of nitrogen

NO_x is mainly the sum of NO and NO_2. The thermal formation of NO emissions can be described via the Zeldovich mechanism and depends on three factors [20] (Wei, Yao, Han, & Pan, 2016): (1) high temperature, (2) high oxygen concentration, and (3) high residence time. The reactions to form NO are $N_2 + O \rightarrow NO + N$ and $N + O_2 \rightarrow NO + O$. Some part of the produced NO further converts to NO_2, predominantly via $NO + HO_2 \rightarrow NO_2 + OH$. The inverse reaction back to NO only occurs if there is a long enough residence time at high temperature. In dual-fuel mode NO_x emissions typically decrease with increasing MEF, but NO_2 emissions generally increase [15] (Coulier & Verhelst, 2016). The generally observed decrease in NO_x emissions is therefore the result of the more dominant decrease of NO emissions in dual-fuel mode. The decrease of NO emissions is attributed to the cooling effect of methanol (resulting in a lower combustion temperature - factor (1)) combined with the more premixed and thus leaner combustion with less near-stoichiometric zones - factor (2).

In [13] (Dierickx, Sileghem, & Verhelst, 2019) it was shown that NO emissions have a parabolic profile in MPI mode at high load: first NO emissions decrease with increasing MEF and then they increase again. The hypothesis was proposed that the parabolic profile is due to a third factor. Namely that due to the largely premixed combustion the temperature rises rapidly - factor (3), causing this third effect to be dominant over factor (1) and (2). From Fig. 18 it can be seen that a similar trend was recorded in SPI mode at 1500 rpm and 10.55 bar. In both modes NO emissions decrease significantly, more specifically decreases between 20% and 80% were recorded, depending on the load, the MEF and depending on the injection mode. The higher the load, the lower the decrease from DO to DF operation. It is assumed that at low load factor (3) is less prominent because the combustion phasing is mainly shifted to later crank angles, in this way causing even higher NO reductions. Also it can be seen that at 7.03 and 10.55 bar bmep the NO emissions are consistently higher in SPI mode than in MPI mode. Comparing the difference between each SPI and MPI measurement results in an average increase of respectively 52% and 26% for 7.03 and 10.55 bar bmep. This can be attributed to the higher temperatures at TDC in SPI as discussed in Section 4.1. For

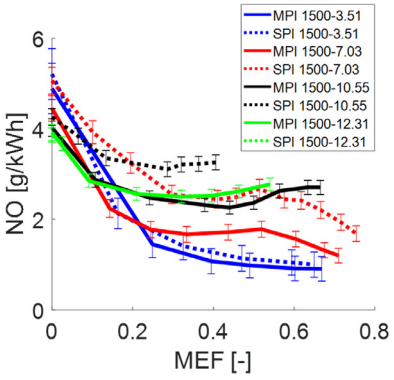

Fig. 18. NO emissions as a function of MEF at 1500 rpm.

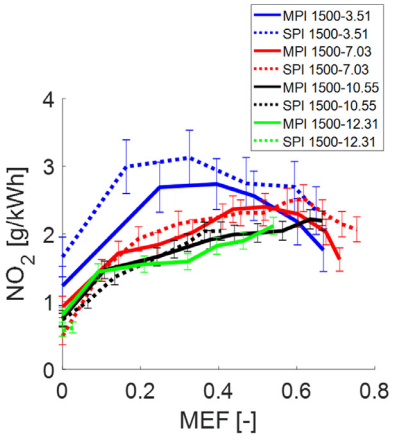

Fig. 19. NO_2 emissions as a function of MEF at 1500 rpm.

the load of 3.51 bar bmep, NO is also slightly higher in SPI, but taking into account the uncertainty this difference is not significant.

As can be seen in Fig. 19, the NO_2 emissions increase in DF mode compared to DO. It can be seen that the most significant absolute increase in NO_2 occurs in SPI mode at 1500 rpm and 3.51 bar. The most significant relative increase of NO_2 compared to DO mode occurs in SPI mode at 7.03 bar bmep where NO_2 increases up to 5 times the value in DO mode. In the other load points NO_2 values are in a range of being a factor of 1.2–2.5 times higher compared to DO. It can also be seen that the NO_2 emissions form a parabolic profile with increasing MEF, except in MPI mode at 10.55 and 12.31 bar bmep where there is a continuous increase with increasing MEF. In literature an increase of NO_2 has been reported. The reason that is given is the more numerous presence of the HO_2 radical. In [21] (Lu, Yao, & Chunde, 2019) the HO_2 mole fraction is calculated via CFD simulations. It was seen that in dual-fuel operation during methanol oxidation significantly more HO_2 is formed than in DO mode, promoting the transformation of NO to NO_2. The decrease in NO_2 at high MEF might be related to a saturation of the NO to NO_2 reaction because of a lack of HO_2 or due to the decreasing availability of NO.

In Fig. 20 the NO_x emissions are shown in SPI and MPI mode at 1500 rpm. It can be seen that the highest decrease rate occurs up to a MEF of around 30%. For MEFs higher than 30% the NO_x emissions further decrease or increase again but this depends on the load. In some points the NO_x emissions even get higher than in DO: at 10.55 bar bmep as of an MEF of 30% and 61% for respectively SPI and MPI, and at 12.31 bar bmep in MPI for an MEF of 52%. In international waters IMO Tier II and III regulations limit NO_x respectively to maximum 7.7 g/kWh and 1.96 g/kWh (= limit for engines with maximum engine speed higher than 2000 rpm).

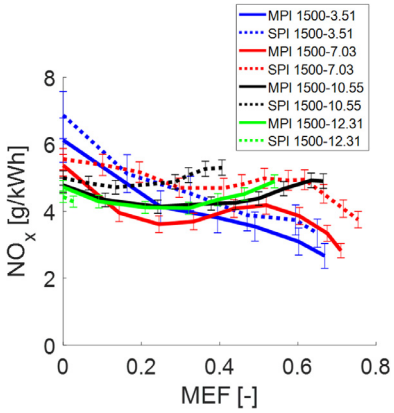

Fig. 20. NO_x emissions as a function of MEF at 1500 rpm.

It can be seen that in DO and both MPI and SPI mode Tier II regulations are met but Tier III is not met. In the majority of the tested load points (44 from 50) NO_x decreases however significantly compared to DO.

5. Discussion

In Section 2 the engine setup of the retrofitted Volvo Penta was discussed along with the technical design requirements of both methanol injection modes. In Section 3 the research methodology was elaborated followed by the experimental results in Section 4. It can now be questioned how the results of this paper can be used for other engine retrofits to dual-fuel operation with methanol-diesel. From the previous sections it can be concluded that several aspects are to be considered when starting retrofit plans.

To enable the choice between MPI and SPI the engine's design first has to be analyzed. If there is an intercooler then it has to be studied whether the cooling power can be controlled and modified to prevent condensation in the intake when injecting methanol at a single point before this intercooler. If not then the intercooler has to be bypassed or dismantled as was done in this research. As was seen in Section 4, the lack of the IC resulted in higher intake temperatures of the methanol-air mixture limiting the substitution boundaries and having a negative impact on NO_x emissions, while a positive impact on efficiency was observed. In future research it would be therefore interesting to test SPI with an intake temperature control mechanism, and as such investigating whether the trade-off between NOx and substitution boundaries on the on hand and efficiency on the other hand can be improved.

For other engine retrofits it can also be withdrawn from this research that the shape of the intake has an important impact on a proper cylinder charge filling. As discussed in Section 4.2.4, methanol droplets are more keen to follow the easiest path. Therefore sharp corners and asymmetric shapes should be avoided to ensure equal filling in all cylinders. Chen et al. [19] (Chen, Yao, & Yao, The impact of methanol injecting position on cylinder-to-cylinder variations in a diesel methanol dual fuel engine, 2017) did not encounter this problem, they have measured similar cylinder-to-cylinder variations in MPI and SPI mode, which could be due to the more symmetric design of the intake manifold of their research engine. For the research in this paper it would be interesting to further investigate this effect, e.g. by modelling the charge flow in the intake manifold.

6. Conclusions

Given that engine retrofitting to dual-fuel operation with methanol-diesel can play an important role in making vessels sus-

tainable, this paper focused on the methanol injection position in the intake and its effect on engine performance, as this position has an important impact on the total retrofit cost. Two methanol injection positions in the intake manifold are possible and were tested: one where methanol is injected just before the inlet valves, at multiple points (MPI mode), and the second where methanol is injected at a single point behind the turbo-compressor (SPI mode). The main difference between both modes is the pathway of methanol before reaching the cylinder and the air-methanol mixing location.

While preparing the measurements it was decided to remove the IC in SPI mode to prevent condensation of methanol in the IC. As a result, the intake charge temperatures are different between MPI and SPI. This has as a consequence that for SPI pre-ignition is observed as an additional diesel substitution boundary compared to MPI. It was concluded though by testing MPI without IC that pre-ignition was independent of the injection mode, but only linked to intake charge temperature.

Five diesel substitution boundaries were observed during the MPI and SPI measurements: partial burn, misfire, knock, excessive exhaust temperatures and pre-ignition. The highest MEF was observed in SPI and amounted to 84%. The max MEF in MPI amounted to 80%. On average higher MEFs can be reached in MPI (the average of all max MEFs (nine tested load points) amount in MPI to 67%, while in SPI to 45%). A higher spread in max MEFs was observed in SPI and this was linked to the higher cylinder-to-cylinder variations, caused by the asymmetric intake manifold of the engine, and to the higher intake charge temperatures causing pre-ignition to occur at low MEFs.

The brake thermal efficiency has been found not to differ significantly between MPI and SPI for low MEFs. At higher MEFs the BTE is higher for SPI than for MPI, for some loads (e.g. at 2000 rpm and 7.03 bar bmep a relative increase of 8.6%). This was ascribed to the higher intake temperatures enabling a better combustion phasing and a slightly more isochoric combustion.

As a result of the higher intake air temperatures, NO_x emissions are higher with SPI than with MPI for the majority of the load points, especially for loads above 3.51 bar bmep. The NO_2 emissions increase with a factor between 1.2 and 2.5 (relatively compared to DO) with increasing MEF depending on the load point, independently of the injection mode – NO_2 differs not significantly between MPI and SPI. NO on the other hand decreases with 20% to 80% with increasing MEF depending on the load, and for loads above 3.51 bar bmep NO is significantly higher for SPI. For both MPI and SPI, NO_x emissions with methanol are lower than NO_x emissions in DO in the majority of the tested load points (44 from the 50).

From this research, it is concluded that from a cost point of view (i.e. maximizing efficiency (and thus minimizing fuel consumption) and minimizing the retrofit cost) SPI is preferred as a retrofit solution for marine vessel engines, but from a sustainability point of view (i.e. maximizing the substitution of diesel by methanol and decreasing NO_x emissions) MPI is preferred.

Finally, it is concluded that an interesting path for future research is to focus on controlling the intake air temperature and the methanol-air mixing. The first to optimize efficiency, to possibly postpone misfire to higher MEFs, and to improve evaporation. The second to ensure a broader stable operating range in DF with low cylinder-to-cylinder variations.

Declaration of Competing Interest

We have no conflicts of interest to disclose

Acknowledgements

The research in this paper has been carried out with the financial support of the Flanders Innovation and Entrepreneurship (Baekeland HBC.2019.2574) in cooperation with Anglo Belgian Corporation NV. The authors wish to acknowledge the European Union's Horizon 2020 research and innovation program for the financial support in LeanShips (Contract No.: 636146), the project leading to this research paper's investigations, and in Fastwater (Contract No.: 860251), a recently started and successor innovation project with amongst other things the aim to demonstrate methanol in real-life vessels.

References

[1] Olah G, Goeppert A, Prakash S. Beyond oil and gas: the methanol economy. 2nd ed. Wiley Online Library; 2009.
[2] Verhelst S, Turner J, Sileghem L, Vancoillie J. Methanol as a fuel for internal combustion engines. Prog Energy Combust Sci 2019;70:43–88.
[3] Verhelst S, Wallner T. Hydrogen-fueled internal combustion engines. Prog Neonoenergy Combust Sci 2009;35:490–527.
[4] Pearson R, Turner J. Renewable fuels – an automotive perspective. Comprehens Renew Energy 2012:1–74.
[5] McGill R, Remley W, Winther K. Alternative fuels for marine applications. IEA Energy Technol Netw 2013.
[6] Yao C, Pan W, Yao A. Methanol fumigation in compression-ignition engines: a critical review of recent academic and technological developments. Fuel 2017;209:713–32.
[7] Bechtold R, Goodman M, Timbario T. Use of methanol as a transportation fuel. Methanol Institute; 2007.
[8] FASTWATER, "FAST track to clean and carbon-neutral WATERborne transport," 2020. [Online] . Available: https://www.fastwater.eu/.
[9] Stojcevski T, Jay D, Vicenzi L. Operation experience of world's first methanol engine in a ferry installation. CIMAC 2016.
[10] Mayer S, Sjöholm J, Murakami T. Performance and emission results from the MAN B&W LGI Low-Speed Engine Operating on Methanol. CIMAC 2016.
[11] LeanShips, "Low energy and near to zero emission ships," 2015-2019. [Online] . Available: https://www.leanships-project.eu/.
[12] Sirimanne S, Hoffmann J. Review of maritime transport. UNCTAD; 2019.
[13] Dierickx J, Sileghem L, Verhelst S. Efficiency and emissions of a high-speed marine diesel engine converted to dual-fuel operation with methanol. CIMAC; 2019.
[14] Chen Z, Yao C, Yao A, Dou Z, Wang B, Wei H, Liu M, Chen C, Shi J. The impact of methanol injecting position on cylinder-to-cylinder variation in a diesel methanol dual fuel engine. Fuel 2017;191:150–63.
[15] Coulier J, Verhelst S. Using alcohol fuels in dual fuel operation of compression ignition engines: a review. CIMAC 2016.
[16] IMO MARPOL/CONF./3.34 – protocol of 1997 and annex VI to MARPOL 73/78 as adopted by the conference. International Maritime Organization; 1997.
[17] Taylor J. An introduction to erro analysis. Sausalito, CA: University Science Books; 1997.
[18] Wang Q, Wei L, Pan W, Yao C. Investigation of operating range in a methanol fumigated diesel engine. Fuel 2015;140:164–70.
[19] Chen Z, Yao C, Yao A. The impact of methanol injecting position on cylinder-to-cylinder variations in a diesel methanol dual fuel engine. Fuel 2017;191:150–63.
[20] Wei L, Yao C, Han G, Pan W. Effects of methanol to diesel ratio and diesel injection timing on combustion, performance and emissions of a methanol port premixed diesel engine. Energy 2016;95:223–32.
[21] Lu H, Yao A, Chunde Y. An investigation on the characteristics of and influence factors for NO2 formation in diesel/methanol dual fuel engine. Fuel 2019;235:617–26.